

Toward an Improved Surface Roughness Parameterization Model for Soil Moisture Retrieval in Road Construction

Thi Mai Nguyen¹, Graduate Student Member, IEEE, Jeffrey P. Walker¹, Fellow, IEEE,
Nan Ye¹, Member, IEEE, and Jayantha Kodikara¹

Abstract—In passive microwave remote sensing, the estimation of the surface roughness parameter is a significant obstacle for soil moisture (SM) retrieval. For a given SM content, the geometric soil surface roughness has been shown to have a large impact on the surface emission at L-band frequency, which affects the SM retrieval success when using the information observed from the radiometer and is represented through the so-called the surface roughness parameter (H_R). Moreover, no previous study has examined the effect of this factor in the context of road construction, where the geometric soil surface roughness is affected by the compaction process, resulting in a substantial change in roughness before and after compaction. Accordingly, a series of experiments at various compaction levels and SM contents was performed for a sand subgrade material in order to identify their effects on H_R . The soil brightness temperature (TB) was measured using an L-band radiometer at different incidence angles and a laser profiler was used to measure the surface roughness standard deviation (σ) before and after compaction. The results of this article have demonstrated that the incidence angle (θ) and SM both affect H_R and its relation to the geometric soil surface roughness. Importantly, these factors are not accounted for by existing models. Consequently, a modified surface roughness parameter (H_R) model, based on the traditional Choudhury model, was developed to include the contribution of these two factors, and its impact on the accuracy of SM retrieval results tested. Specifically, it was shown that it is possible to obtain SM retrieval results with an accuracy of $0.04 \text{ cm}^3/\text{cm}^3$ at almost all incidence angles using either dual-polarization [both horizontal (H) and vertical polarization (V)] or only vertical polarization observations. The modified surface roughness parameter (H_R) model has improved the performance of the SM retrieval model to achieve an accuracy of $0.04 \text{ cm}^3/\text{cm}^3$, whereas the traditional Choudhury model achieved an accuracy of only $0.05 \text{ cm}^3/\text{cm}^3$.

Index Terms—L-band radiometer, sand subgrade, soil moisture (SM), surface roughness parameter.

Manuscript received 2 October 2022; revised 2 December 2022 and 18 December 2022; accepted 12 January 2023. Date of publication 20 January 2023; date of current version 1 February 2023. This work was supported in part by the Smart Pavements Australia Research Collaboration (SPARC) Hub at the Department of Civil Engineering, Monash University, under Project IH18.03.2; in part by the Australian Research Council (ARC) Industrial Transformation Research Hub (ITRH) Scheme under Project IH180100010; in part by Construction, Infrastructure, Mining and Concessions (CIMIC); and in part by the Engineering, Innovation and Capability (EIC). (Corresponding author: Thi Mai Nguyen.)

The authors are with the Department of Civil Engineering, Monash University, Clayton, VIC 3800, Australia (e-mail: thi.nguyen9@monash.edu).

Digital Object Identifier 10.1109/TGRS.2023.3238367

I. INTRODUCTION

COMPACTION is one of the most critical aspects in pavement construction, as failure to achieve optimum compaction can result in serious impacts on the pavement performance. For a given compaction effort, the maximum dry density is reached at what is called the optimal moisture content, resulting in optimum compaction. For this reason, soil moisture (SM) plays a key role in compaction during pavement construction. Currently, it is difficult to monitor the variation in SM content along construction corridors since most sampling methods are conducted manually at a few isolated locations [1]. However, radiometer measurements at L-band (1–2 GHz) have been shown to provide the most precise approach to remote SM retrieval in agricultural fields [2], [3]. Nguyen et al. [4] demonstrated the ability of using an L-band radiometer for SM retrieval for typical road construction materials. Specifically, the retrieval results have achieved an accuracy of $0.05 \text{ cm}^3/\text{cm}^3$ for the sand subgrade material. However, L-band radiometer data from space have been specified to provide a target SM retrieval accuracy of up to $0.04 \text{ cm}^3/\text{cm}^3$ in agricultural applications [5], [6], [7]. In addition, recent ground-based SM measurement studies have successfully achieved the SM retrieval accuracy of approximately or less than this target [8], [9], [10], which means that the retrieval result for the sand subgrade material can potentially be further improved. Accordingly, this article is a follow-up in a series of papers exploring a new method for monitoring the spatial variation of SM in road construction applications.

For a given SM condition at L-band, vegetation water content (VWC), soil effective temperature, and soil surface roughness have the greatest impact on the surface emission at microwave wavelengths. In road construction, the effect of vegetation can be ignored, and therefore, the choice of the parameters used to model the effect of geometric soil surface roughness on the emission is of primary importance. A wide variety of solutions are available for rough surface microwave radiation such as the approximate Kirchhoff theory and small perturbation method [11], integral equation model (IEM) [12], advanced IEM (AIEM) [13], a recently proposed surface roughness formulation [14], and the most commonly used semiempirical Q/H model [15]. Accordingly, Nguyen et al. [4]

TABLE I
MAJOR ROUGHNESS PARAMETERIZATION SCHEMES AND THEIR LIMITATIONS

Surface roughness parameter model	Key research points	Knowledge gap	Authors
$H_p = \exp[-(2k * \sigma)^2 * \cos^2 \theta]$, where H_p is the roughness effect, k is the wavenumber expressed as $k = 2\pi/\lambda$, λ is the wavelength, and θ is the incidence angle.	An early attempt to relate the roughness parameter to σ .	Previous studies have indicated that the roughness parameter value obtained from this model is generally overestimated for rough soils [24], [25], which is characteristic of the surface roughness in road construction.	Choudhury et al., 1979 [23]
$H_p = \exp(-G) = \exp[\ln(S(\theta)f(k\sigma, kLC, \theta))]$, where G is a roughness attenuation parameter, $S(\theta)$ is a shadowing function and $f(k\sigma, kLC, \theta)$ is a function of the wavenumber (k)	Simulated the effects of surface roughness on the effective surface reflectivity and found that the roughness parameter depends on SM and the ratio of σ/LC , and it varies with the incidence angle (θ) and polarization (p).	This parameterization was not fully validated because three different roughness conditions were used, whose surface roughness profiles were obtained over the fields by driving gridded panels into the soil and taking photos at only two different locations for each of the three bare plots [26]. More accurate roughness profile measurement data is needed in order to properly characterize the surface roughness condition.	Mo and Schmugge, 1987 [18]
$H_p = \exp[-(\alpha - \delta * SM)m^\beta]$, where $m = \sigma/LC$ and α, β, δ are adjustable parameters (depending on θ and p)	Developed an empirical rough surface reflectivity model using ground radiometer measurements. The reported accuracies of the surface reflectivity in terms of the random-mean-square errors (RMSE) were 0.095 and 0.061 for H and V polarizations, respectively.	Data used in this study was obtained over a wide frequency range (2 - 94 GHz), which does not include the L-band. Also, the main limitation of the model was the incomplete characterization of the surface roughness effect on the microwave reflectivity by using only σ .	Wegmuller and Matzler, 1999 [27]
$H_p = \exp[-(0.5761 * SM^{-0.3475}) * (\sigma/LC)^{0.4230}]$	Developed an empirical rough surface reflectivity model using experimental measurements over different roughness conditions at L-band and $\theta < 40^\circ$. An empirical model was also developed expressing the roughness parameter as a function of combinations of the variables σ, LC , and SM.	In this experimental dataset, the roughness conditions did not change much during the radiometric measurements and so only a very narrow set of roughness conditions were tested.	Wigneron et al., 2001 [19]
$H_p = \exp[-1.3972 * (\sigma/LC)^{0.5879}]$	Suppressed the dependence on SM with a best fit formulation of the roughness parameter developed. The reported RMSE for the surface reflectivity was 0.031. This study concluded that the roughness parameter is independent of both θ and p .		Wigneron et al., 2001 [19]
$H_p = \exp[-(0.9437 * \sigma) / (0.8865 + 2.2913 * \sigma^6)]$	Developed an empirical power function relating the retrieved values of the roughness parameters. A good accuracy (better than 5 K) over a large range of soil roughness and SM condition was achieved when using this new calibration of the retrieval model.	The model was derived from a unique dataset where the SM was measured over the top 2 cm of the soil instead of over the top 5 cm, which may affect the observed SM dependence of the roughness parameter.	Wigneron et al., 2010 [24]
$H_p = \exp\left[-2.615 * \left(1 - \exp\left(-\frac{Z_s}{2.473}\right)\right)\right]$ if $Z_s < 1.235$, and $H_p = \exp(-1.0279)$ if $Z_s > 1.235$, where $Z_s = \sigma^2/LC$	Developed a numerical model for the roughness parameter over bare soil. In addition, the roughness parameter was found to have a negligible dependence on SM.	The parameter was fitted using limited measurements in an agriculture field. It, therefore, cannot cover and adequately describe the roughness characteristic of road construction; making it improbable to consider using this model in the field of road construction.	Lawrence et al., 2013 [28]
$H_p = G_R = \exp[-\delta_R^2 * (c_0 + c_1 * \tau_F(p, \theta)) * \cos^2(\theta) * 1000]$, where G_R is the reflection reduction factor, τ_F is Fresnel power reflection coefficient, δ_R is the height of matching layer, and c_n is the parameterization constant	Proposed a roughness model using a matching layer and a random depolarizer to describe bare soil surface roughness. Moreover, the roughness parameter showed dependence on θ and a very low sensitivity to roughness for brightness temperature (TB) measurements at V polarization.	The model has been tuned using a small set of measurements and only a few photographed surface profiles in each field were taken. Therefore, a more accurate characterization of the surface roughness profiles in terms of length and number of samples is necessary.	Goodberlet and Mead, 2013 [29]
$H_p = A_p * \exp(B_p * m^2 + C_p * m)$, where $m = \sigma^2/LC$, $A_p, B_p, C_p = a * SM^2 + b * SM + c$, a, b, c for both V and H polarizations were listed	Expressed the roughness parameter as an exponential function of a defined slope parameter (m). The achieved accuracies for SM retrieval were 0.03 m ³ /m ³ and 0.04 m ³ /m ³ for ascending and descending orbits, respectively.	The model was developed from the viewpoint of theoretical simulations with L-band observations obtained at satellite scale. Accordingly, the dataset and an accurate estimation of the surface characteristics from a large number of field scale observations are essential to validate the feasibility of the model for small scale studies in general and road construction in particular.	Zhao et al., 2015 [30]

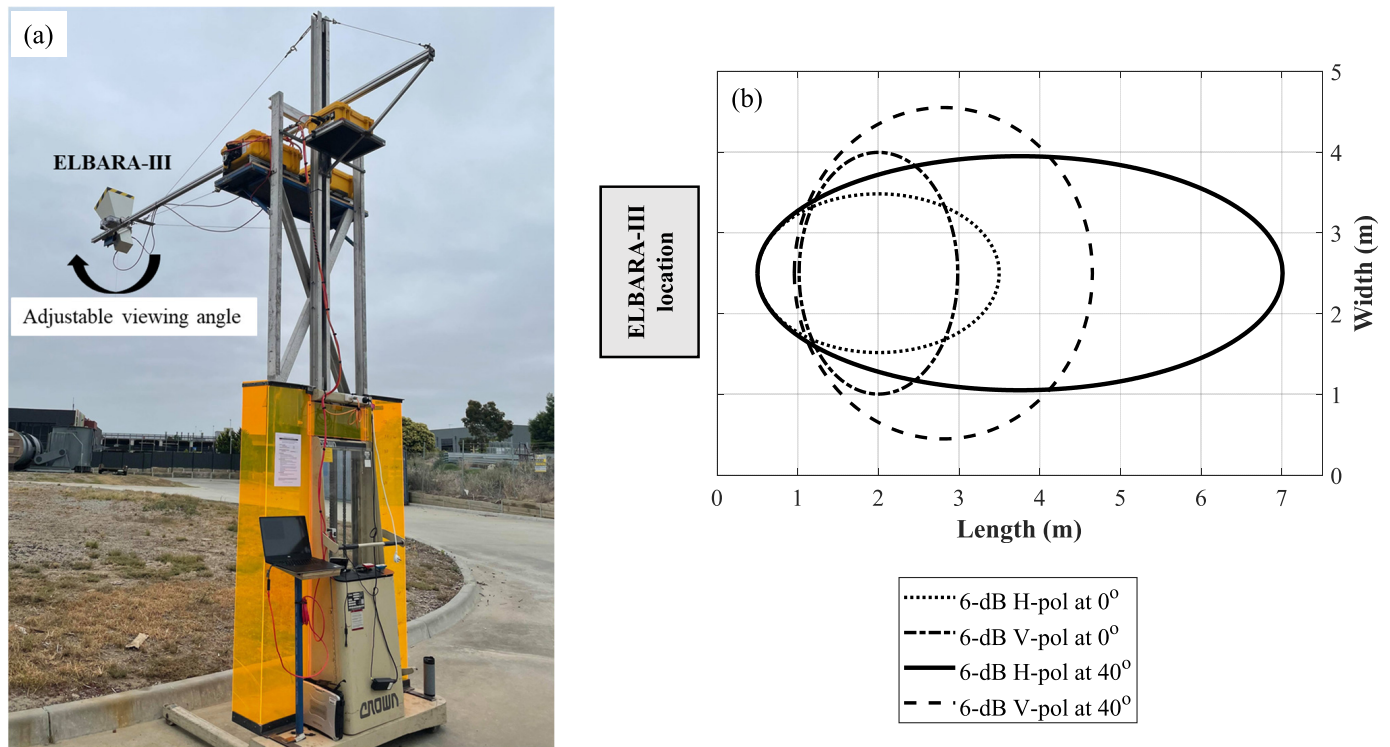


Fig. 1. Photograph showing (a) electronic hoist used to support the ELBARA-III system and (b) footprint of ELBARA-III at 0° and 40° incidence angles. The horn’s antenna viewing angle could be adjusted in 5° steps from 0° to 180°.

used the Q/H model to describe the emissivity of a bare surface. Generally, the semiempirical Q/H model has been used to parameterize the surface roughness, which describes the effect of surface roughness on the microwave emission, including two best-fit parameters Q_R and H_R [15], and define H_R dependent on the incidence angle using N_R [16]. H_R is typically estimated based on measurable geophysical characteristics of the surface [standard deviation of heights (σ) or autocorrelation length (LC)]. In passive microwave measurements, Q_R is a parameter for polarization mixing. While Q_R depends on the electromagnetic frequency, its value has been found to be very small at L-band [17] and has been taken as 0 in many studies [18], [19]. N_R is the angular dependence, and based on long-term measurements, a subsequent study has found that $N_R \approx 1$ at horizontal (H) and $N_R \approx -1$ at vertical (V) polarization over bare fields [20]. Nonetheless, H_R is not well understood in relation to surface roughness characteristics, being observed to decay linearly with increasing SM between a transition SM point and the field capacity (FC) while remaining constant outside those limits [20], [21], [22].

A number of surface roughness parameter models have been developed for agricultural applications; it is, however, difficult to confidently apply these models in road construction applications due to the limitations listed in Table I. Moreover, no previous research has explored the impact of H_R on surface emission at the L-band in road construction. In this context, the soil surface is affected by the compaction process, leading to a substantial change in geometric soil surface roughness before and after soil compaction. Moreover, the soil compaction

caused by heavy machinery not only increases the soil bulk density [31], [32] but subsequently results in changes in volumetric moisture content (VMC), which is the key parameter to be observed by the radiometer. Consequently, the roughness effect can be complex and influenced not only by the geometric soil surface roughness but also the wavelength (k), polarization (p), incidence angle (θ), and changes in bulk density (ρ_b) [30] during compaction. As a result of these synergistic effects, the notion that H_R depends purely on geometric soil surface roughness is challenged. In addition, to estimate the surface characteristics accurately, a large number of surface roughness observations are required (i.e., sample interval and profile length) [33], [34], and this requirement cannot be met easily over a large area (i.e., agricultural field or stretch of road construction). Accordingly, this article examined and evaluated the impact of different factors on H_R including SM and incidence angle (θ) rather than only considering the surface geophysical shape; using observations at L-band, supported by ancillary data and intensive surface roughness measurements for different compaction scenarios, surface roughness conditions, and SM contents.

II. DATASETS

This study used an L-band third-generation portable ground-based passive radiometer system commissioned by the European Space Agency [35] called ELBARA-III to measure the brightness temperature (TB) of the soil surface [Fig. 1(a)]. The roughness measurement technique used in this study was a laser-based distance sensor that does not damage the fragile surface, which can lead to an error when having direct contact

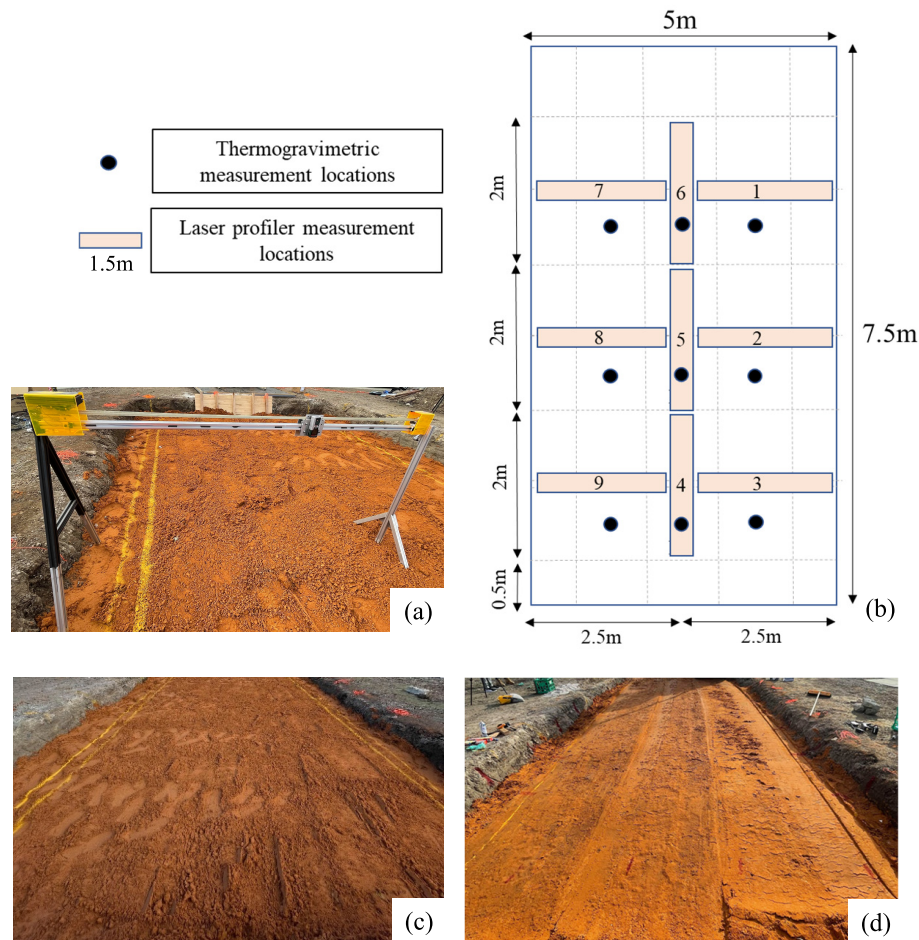


Fig. 2. Photographs illustrating use of (a) laser profiler to measure the surface roughness and (b) nine locations of surface roughness measurement and thermogravimetric ring measurements. Also shown is the sand surface (c) before and (d) after the compaction process.

with the measuring device. The laser profiler is the noncontact technique [36], recording the surface profile using a laser beam that measures the distance between a horizontally positioned rail and a carriage. Accordingly, the surface roughness was measured using a laser profiler at nine locations with different orientations, with the recommended 3-m roughness profiles [37] created by combining two 1.5-m-long transects (Fig. 2). Other equipment used to collect data required by this experiment included Stevens Water Hydra-Probes for measuring soil temperature and SM profiles at 5-cm depth increments and thermogravimetric ring measurements that measured top 5-cm SM variation at nine locations across the testbed for independent validation.

To cover the footprint of the radiometer [see Fig. 1(b)], a testbed with dimensions of 5 m (width) \times 7.5 m (length) was constructed. The experiment was performed at different levels of compaction and SM content for two 30-cm-thick layers of sand subgrade in the testbed. A concrete batching plant was used to homogenize the material and then compacted layer by layer using a 4.5-ton double drum roller. Photographs of the soil surface before and after compaction are shown in Fig. 2. Before and after compaction, ELBARA-III was used to measure the soil TB at different angles (0° – 40° at 5° steps)

followed by the roughness and ancillary measurements. After compacting to 30 cm, surface watering was performed with two sprinklers to provide additional SM contents up to FC of the material. The photograph of the roller used for soil compaction and surface watering using sprinklers is shown in Fig. 3.

Six sets of experiments were conducted, each with two layers of compacted soil at different SM contents, with two of these sets of experiments having surface watering afterward. In total, data were collected for six experiments before compaction, six experiments after compaction, and two experimental lots after watering. Table II shows the SM content details for each experimental day.

III. METHODOLOGY

The steps to implement the forward model used to predict the TB of the soil surface, and the inversion algorithm to retrieve the SM, are detailed in [4]. In summary, a forward model was established to predict TB, with the reflectivity (r) of the soil surface calculated using the Fresnel equations [38] based on the dielectric constant obtained from the dielectric mixing Dobson model [39], and the incidence



Fig. 3. Photographs showing (Left) compacting of the soil using a roller and (Right) watering of the surface using sprinklers.

TABLE II
DETAILS OF TESTING TIME AND SM CONTENT IN EACH EXPERIMENTAL DAY

	Date	SM (cm ³ /cm ³) before compaction (at top 5 cm)	Dry density (g/cm ³) (at top 5 cm)	SM (cm ³ /cm ³) after compaction (at top 5 cm)	Dry density (g/cm ³) (at top 5 cm)
Layer 1	29-Jul, 2021	0.19	1.53	0.22	1.92
	14-Sep, 2021	0.20	1.38	0.23	1.75
	01-Feb, 2022	0.08	1.20	0.13	1.89
Layer 2	30-Jul, 2021	0.19	1.54	0.21	1.83
	16-Sep, 2021	0.19	1.43	0.23	1.79
	02-Feb, 2022	0.10	1.31	0.12	1.78
Watering the surface (at the field capacity)	10-Aug, 2021	-	-	0.27	1.96
	02-Feb, 2022	-	-	0.17	1.85

angle (θ), for H and V polarizations. The semiempirical Q/H model [15], which defines H_R dependent on the incidence angle and polarization [16], was then used to obtain the rough surface reflectivity. The simple linear parameterization given by Choudhury et al. [40] was adopted to relate the soil surface and deep temperature through a parameter named the soil effective temperature (T_{eff}). Accordingly, the TB of the bare soil surface was simulated based on the soil effective temperature and the rough surface reflectivity. Finally, a cost function (CF), derived from the L-band microwave emission of the biosphere (L-MEB) inversion model [41], was used to retrieve the SM or H_R by iteratively running the forward model to match with the known TB observed from ELBARA-III. The forward model requires seven input parameters, including SM(cm³/cm³), surface roughness parameter (H_R), bulk density [ρ_b (g/cm³)], sand (S) and clay (C) fraction, and the soil surface [T_{surf} (K)] and deep [T_{deep} (K)] temperature at 5 and 40 cm depth, respectively. In this article, the local sensitivity method for sensitivity analysis was used. The main content of this analysis was to vary input parameters of the TB simulation model based on their defined range of values for a particular material (sand subgrade). The result was the effect on TB when changing these factors. Accordingly, the sensitivity of the simulated TB to input variations was estimated to determine the factor that has the most influence on the retrieval results by varying these parameters.

The surface roughness parameter (H_R) model proposed by Choudhury et al. [23], having a dependence of H_R on the standard deviation (σ) of the surface height, was used and estimated as

$$H_R = (2k * \sigma)^2. \tag{1}$$

The radio-brightness model presented in [4] can be used to retrieve SM or H_R as an unknown parameter using observed TB from the ELBARA-III and measured value of H_R or SM, respectively. In order to examine the relationship between the surface roughness parameter (H_R) and the change in incidence angle, H_R was first retrieved from the inversion of the radio-brightness model as an unknown parameter (i.e., retrieval) using measured values of SM. H_R was then calculated from the Choudhury model using geometric soil surface roughness data measured from the laser profiler. Accordingly, the correlation between H_R results obtained from the inversion (retrieval) of the radio-brightness model and calculated from the Choudhury model at different incidence angles was analyzed.

At L-band, soil roughness is more affected by the distribution of water in the top layer than the purely geometric soil surface roughness, which dominates only when the soil is in a very wet condition [42]. The roughness effects have also been shown to be a power function of SM [19], [22], [43], [44], which has been demonstrated at satellite scale over some regions [45]. To prove this point, the soil water

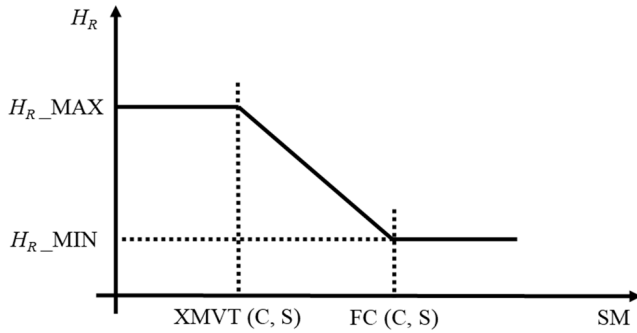


Fig. 4. Simple law expressing the surface roughness parameter (H_R) as a piecewise function of SM [42]. The principle of soil water contribution to H_R with a transition moisture point, XMVT (C, S) and the FC (C, S). H_{R_MIN} and H_{R_MAX} are the roughness parameters calculated from the Choudhury model and obtained from the inversion (retrieval) of the radio-brightness model, respectively.

contribution to H_R was considered, with the view to having H_R as a function of SM according to the simple law shown in Fig. 4. Accordingly, below a transition moisture point, XMVT (C, S), and above the FC (C, S), the roughness parameter takes the classical expression ($H_{R_MIN} = ((2k\sigma)^2)$ [23]. The two parameters XMVT and FC are the function of the sand (S) and clay (C) fractions. The computation of those values was discussed in detail in [46]. Specifically, from S and C fractions, the transition moisture (XMVT) can be computed. First, the wilting point [WP (C, S)] is expressed by

$$WP(C, S) = CWP1 + CWP2*S + CWP3*C \quad (2)$$

where $CWP1 = 0.06774$, $CWP2 = -0.00064$, and $CWP3 = 0.00478$, and the final transition moisture [XMVT (C, S)] is calculated as

$$XMVT(C, S) = CXMVT1*WP(C, S) + CXMVT2 \quad (3)$$

where $CXMVT1 = 0.49$ and $CXMVT2 = 0.165$. The FC is defined by

$$FC(C, S) = 0.03 - 0.0023*S + 0.005*C. \quad (4)$$

The sand subgrade material used in this study has the fraction of sand and clay as 0.88 and 0.0093, respectively.

The H_{R_MAX} value for dry soil could be set a priori and/or adjusted from the data. Thus, H_{R_MAX} was the retrieval parameter from all nine incidence angles at different SM contents. The model was developed using data from the first layer and after watering on August 10, and its performance was validated using data from the second layer and after watering on February 2. Using linear regression, the Choudhury model has been modified in this article to include the effects of incidence angle and SM rather than just pure geometric soil surface roughness. Finally, the observed TB from ELBARA-III at different angles, together with ancillary measurements such as surface roughness, soil temperature, and soil texture, was used to retrieve the VMC of the compacted soil using both the original Choudhury and modified H_R models. SM content measured using traditional techniques (thermogravimetric ring measurement) at targeted locations was used to validate the result and compare the performance of the two roughness models. Different approaches to retrieve SM, such as using

single (H or V) or dual (H and V) polarizations, were investigated and their results were compared.

IV. RESULTS

A. Sensitivity Analysis of SM Retrieval to the Input Parameters

In order to determine which input parameter has the most impact on the retrieval results, a local sensitivity analysis of input parameters to the simulated TB was conducted. The value range of input parameters was established based on their actual values obtained from experiments in this study. The following points can be observed in Fig. 5.

- 1) The surface roughness parameter (H_R) had the greatest influence on TB with a change of 0.1 in H_R leading to a change of 5 K in TB.
- 2) An increase of 0.1 in sand (S) fraction led to a decrease of 2 K in TB.
- 3) Compared to the effect of sand (S) fraction, the change of clay (C) fraction does not show much impact on the change of the simulated TB.
- 4) A change of 0.01 g/cm^3 in bulk density (ρ_b) between 1 and 1.5 g/cm^3 led to a 3 K increase in TB, while a change of ρ_b in the range of 1.5–2.5 g/cm^3 did not have any effect on TB.
- 5) Every 1 K increase in soil surface temperature (T_{surf}) led to an approximately 0.6 K increase in TB.
- 6) The change of soil deep temperature (T_{deep}) did not have any effect on TB for the tested set of conditions.
- 7) Finally, the increase in TB resulted in an increase in SM of approximately 0.0086 cm^3/cm^3 per K.

In summary, it was found that H_R , S fraction, and T_{surf} had a greater effect on the change of TB compared to C fraction, ρ_b , and T_{deep} , with H_R being the factor having the greatest effect on the TB simulation result. It can be seen in Fig. 5(d) that the effect of ρ_b on TB varied with the change of ρ_b range value (e.g., TB increased when ρ_b changed from 1 to 1.5 g/cm^3 and TB decreased when ρ_b changed from 1.5 to 2.5 g/cm^3). Accordingly, the impact of H_R , S fraction, ρ_b , and T_{surf} was tested at two SM conditions (wet condition with $SM = 0.5 \text{ cm}^3/\text{cm}^3$ and dry condition with $SM = 0.1 \text{ cm}^3/\text{cm}^3$). The results in Fig. 6 show that at a high SM condition, H_R had a greater effect on TB [Fig. 6(a)], with the opposite being true for S fraction [Fig. 6(b)] and ρ_b [Fig. 6(c)]. The effect of T_{surf} on TB was unchanged under different SM conditions [Fig. 6(d)]. Roughness was again found to be the most influential factor, with variations in H_R causing a 120 K difference in TB under wet conditions, with the effect being greatly reduced in dry conditions having a 55 K change in TB. When the S fraction varied from 0 to 1, the TB changed by 25 K in dry conditions and only 10 K in wet conditions. ρ_b had the least impact, with a change in ρ_b resulting in a TB change of less than 5 K under varied SM conditions. Accordingly, H_R was the parameter having the greatest impact on the TB simulation result, providing impetus to focus on roughness estimation.

B. Improved Surface Roughness Model

Fig. 7 shows the H_R results obtained from both inversions (retrieval) of the radio-brightness model and as calculated from

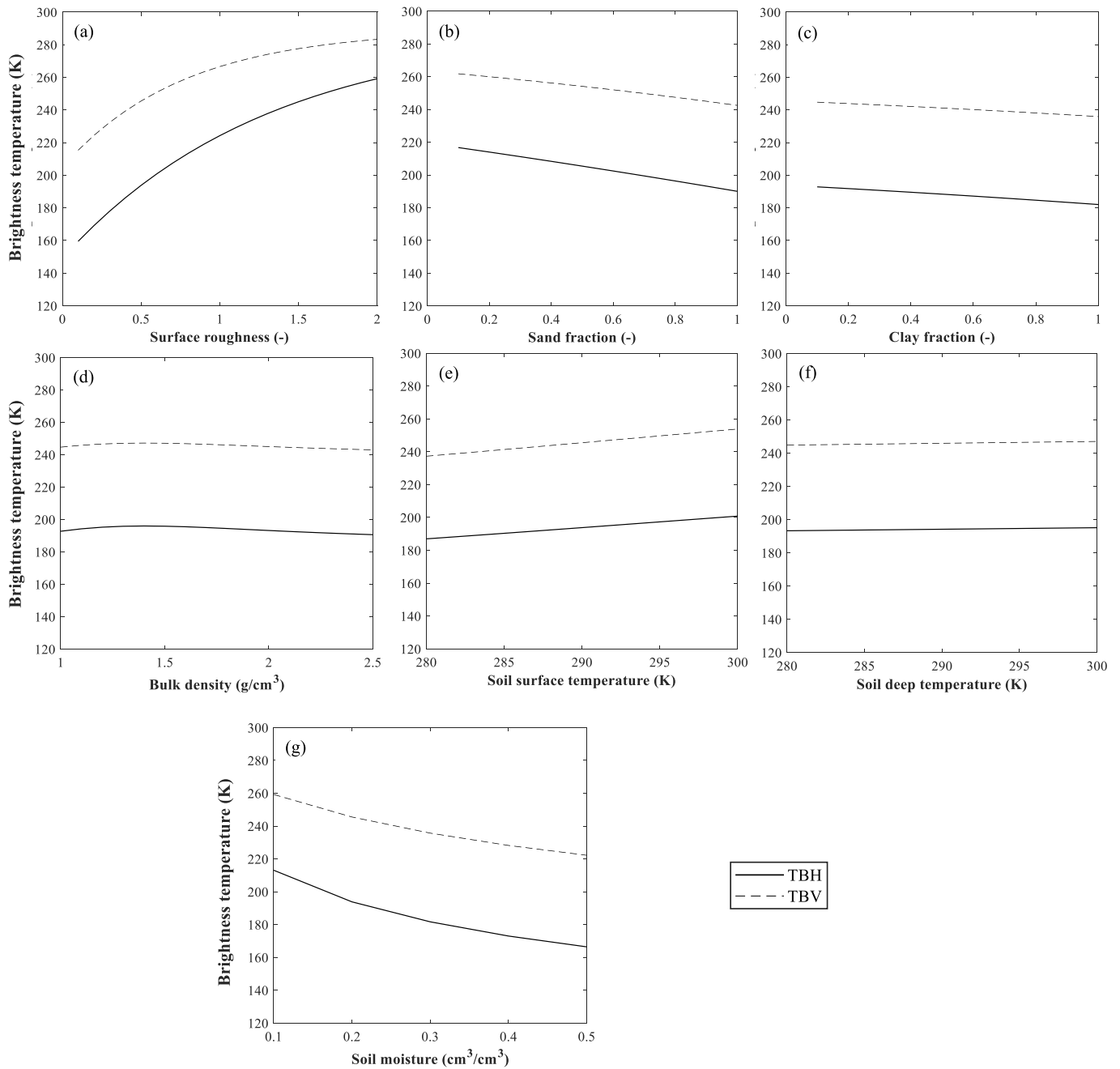


Fig. 5. Sensitivity of TB (K) to (a) surface roughness parameter (H_R) varying from 0 to 2, (b) sand (S) and (c) clay (C) fraction varying from 0 to 1, (d) bulk density (ρ_b) varying from 1 to 2.5 g/cm³, (e) soil surface (T_{surf}) and (f) deep temperature (T_{deep}) varying from 280 to 300 K, and (g) SM varying from 0.1 to 0.5 cm³/cm³. All calculations are for nominal values of SM = 0.2 cm³/cm³, incidence angle = 40°, H_R = 0.5, S = 0.88, C = 0.01, ρ_b = 1.9 g/cm³, T_{surf} = 290 K, and T_{deep} = 286 K.

the Choudhury model at different incidence angles. As the incidence angle increased from 0° to 40°, the retrieved H_R from the radio-brightness model decreased before compaction, while remaining almost unchanged after compaction as the geometric soil surface roughness remained the same. Moreover, the H_R retrieval on August 10 was a constant value at all angles as the SM content reached the FC of the material. The relationship between the H_R results obtained from these two models at different incidence angles is presented in Fig. 8 and Table III. The results show that there is a stronger agreement

between the two values before compaction, with $R^2 > 0.86$ at angles ranging from 0° to 25°, demonstrating that before compacting the soil, H_R is highly influenced by geometric soil surface roughness. However, this consensus is almost absent in the compacted soil ($R^2 < 0.1$ except at 5°), suggesting that there are factors other than angle that also need to be considered.

Because the geometric soil surface roughness varies from experiment to experiment before compaction, H_R is observed to be dependent on geometric soil surface roughness

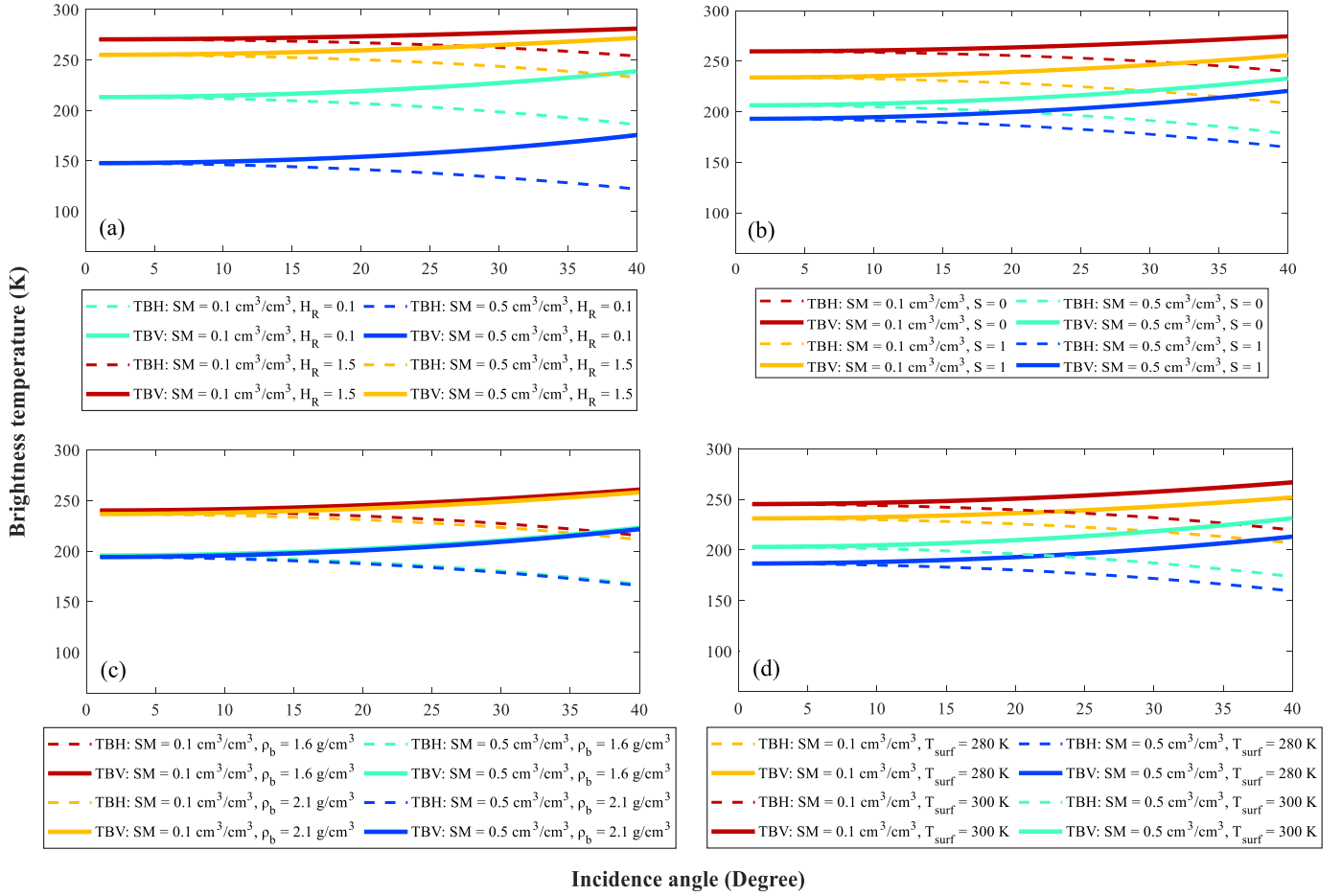


Fig. 6. Sensitivity of TB (K) to (a) surface roughness parameter (H_R), (b) sand fraction (S), (c) bulk density (ρ_b), and (d) soil surface temperature (T_{surf}) at different SM conditions and incidence angles for a base scenario of $H_R = 0.5$, $S = 0.88$, $C = 0.01$, $\rho_b = 1.9 \text{ g/cm}^3$, $T_{surf} = 290 \text{ K}$, and $T_{deep} = 286 \text{ K}$.

TABLE III

R^2 BETWEEN H_R IN FIG. 8 OBTAINED FROM THE INVERSION (RETRIEVAL) OF THE RADIO-BRIGHTNESS MODEL AND FROM THE CHOUDHURY MODEL AT NINE DIFFERENT INCIDENCE ANGLES (FROM 0° TO 40°) BEFORE AND AFTER THE COMPACTION PROCESS

Incidence angle ($^\circ$)	0	5	10	15	20	25	30	35	40
Before compaction (R^2)	0.94	0.95	0.95	0.94	0.87	0.86	0.68	0.5	0.72
After compaction (R^2)	0.071	0.24	0.067	0.087	0.047	0.018	0.042	0.052	0.047

(surface height), while the compacted surface typically has a consistently smooth surface finish with geometric soil surface roughness being the same. Therefore, a relationship was built between changes in H_R obtained from the inversion (retrieval) of the radio-brightness model, the Choudhury model, and SM to examine the impact of SM on H_R for the compacted soil. This analysis used the data measured on February 1, February 2, July 29, September 16, and August 10 after compaction representing days when SM varied from dry to FC condition with a VMC of 0.12, 0.17, 0.22, 0.23, and $0.27 \text{ cm}^3/\text{cm}^3$, respectively. The inversion of the radio-brightness model was used to retrieve H_R as an unknown parameter and the Choudhury model was used to calculate H_R based on laser profiler measurements of surface roughness. These H_R values were then expressed together with the

corresponding SM values in each experimental day (Fig. 9). This result shows the dependence of H_R on the change of SM when the geometric soil surface roughness is unchanged, which is consistent with the simple law (as indicated in Fig. 4) showing H_R as a piecewise function of SM [42]. Specifically, H_R was constant from dry condition to a transition moisture point ($\text{XMVT} = 0.198 \text{ cm}^3/\text{cm}^3$) and decreased from XMVT to the FC ($= 0.28 \text{ cm}^3/\text{cm}^3$). Moreover, after FC, the inversion (retrieval) of the radio-brightness model produced the same H_R value ($H_R = 0.3$) as the Choudhury model, indicating that under very wet conditions, H_R completely depends on geometric soil surface roughness.

Utilizing different models to account for the effect of SM or incidence angle to acquire H_R for various compaction situations is not practical for operational application. Thus, the

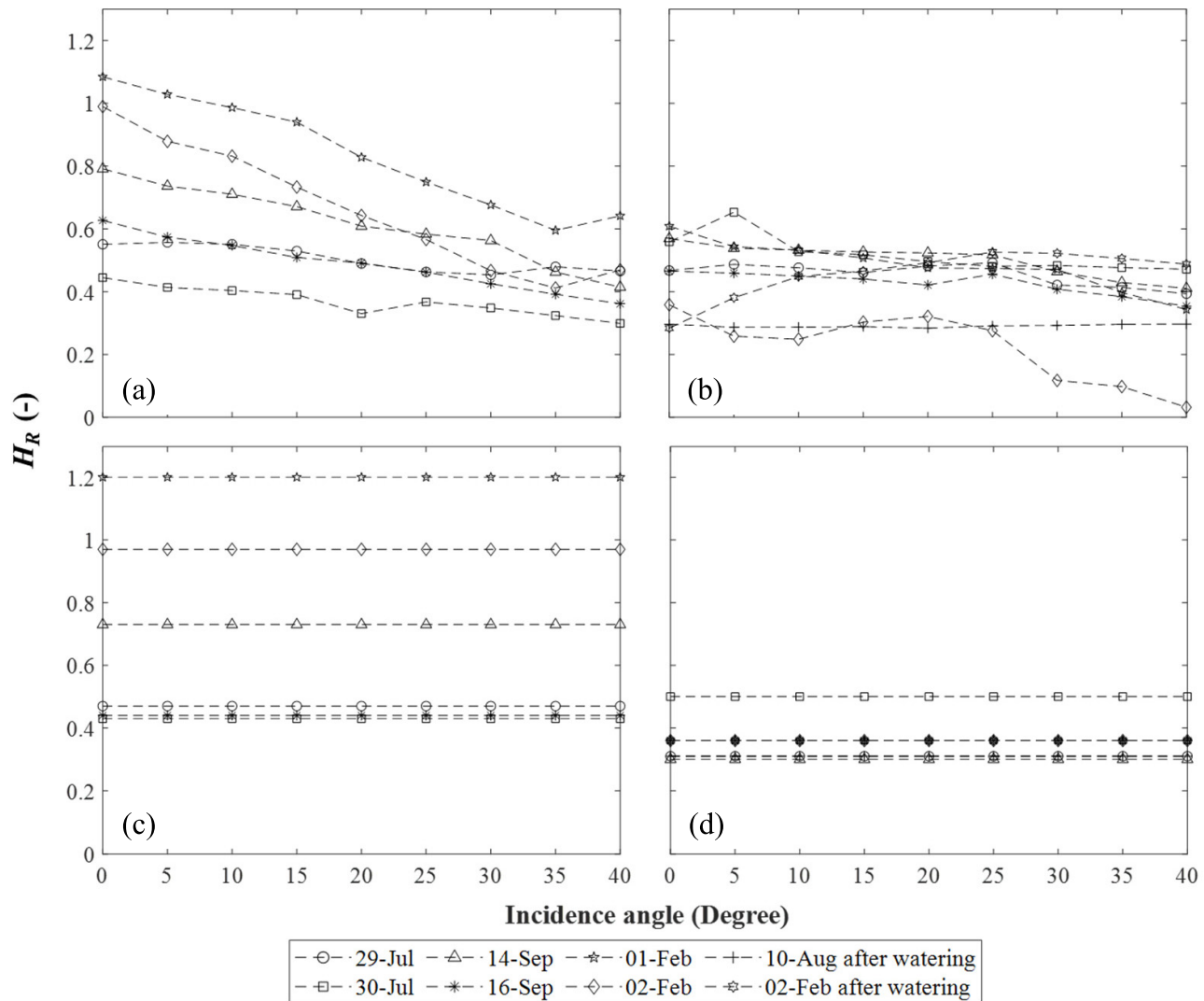


Fig. 7. H_R values obtained from the inversion (retrieval) of (a) and (b) radio-brightness model and (c) and (d) Choudhury model at nine different incidence angles (from 0° to 40°) before [(a) and (c)] and after [(b) and (d)] the compaction process.

Choudhury model was modified utilizing linear regression, with application to both before and after compaction. This surface roughness parameter (H_R) model considered factors other than geometric soil surface roughness (surface height) influencing H_R , including SM and incidence angle (θ). The model was developed using data from the first layer experiments, including before and after compaction and the data after watering on August 10, resulting in

$$H_R = ((1.77 - 0.009 \cdot \theta + 2.8 \cdot SM) \cdot k \cdot \sigma)^2. \quad (5)$$

The data of the second layer, including before and after compaction and the data after watering on February 2, were used to validate the performance of the modified H_R model. The results in Fig. 10 show a clear improvement in the correlation between H_R obtained from the inversion (retrieval) of the radio-brightness model and that obtained when using the modified H_R model ($R^2 = 0.634$) instead of the Choudhury model ($R^2 = 0.539$).

C. SM Retrieval

The constant H_R value obtained from the Choudhury model, which only includes geometric soil surface roughness, was first used as the input parameter to retrieve SM at each incidence angle for six sets of experiments before and after the compaction process of the second layer and after surface watering on February 2. By comparing the root mean square error (RMSE) of the different retrieval approaches—using single (H or V) or dual (H and V) polarizations—the SM retrieval accuracy when using two polarizations (H and V) and V polarization was found in Fig. 11(a) to provide better accuracy than using H polarization. The accuracy was consistently around $0.05 \text{ cm}^3/\text{cm}^3$ for the angle range from 0° to 15° but increased as high as $0.12 \text{ cm}^3/\text{cm}^3$ at 35° . After using H_R values obtained from the modified H_R model as the input parameter to retrieve SM at each incidence angle for the same dataset, the accuracy of the SM retrieval at dual polarizations and V polarization was found to still outperform results from H polarization, as shown in Fig. 11(b). In addition,

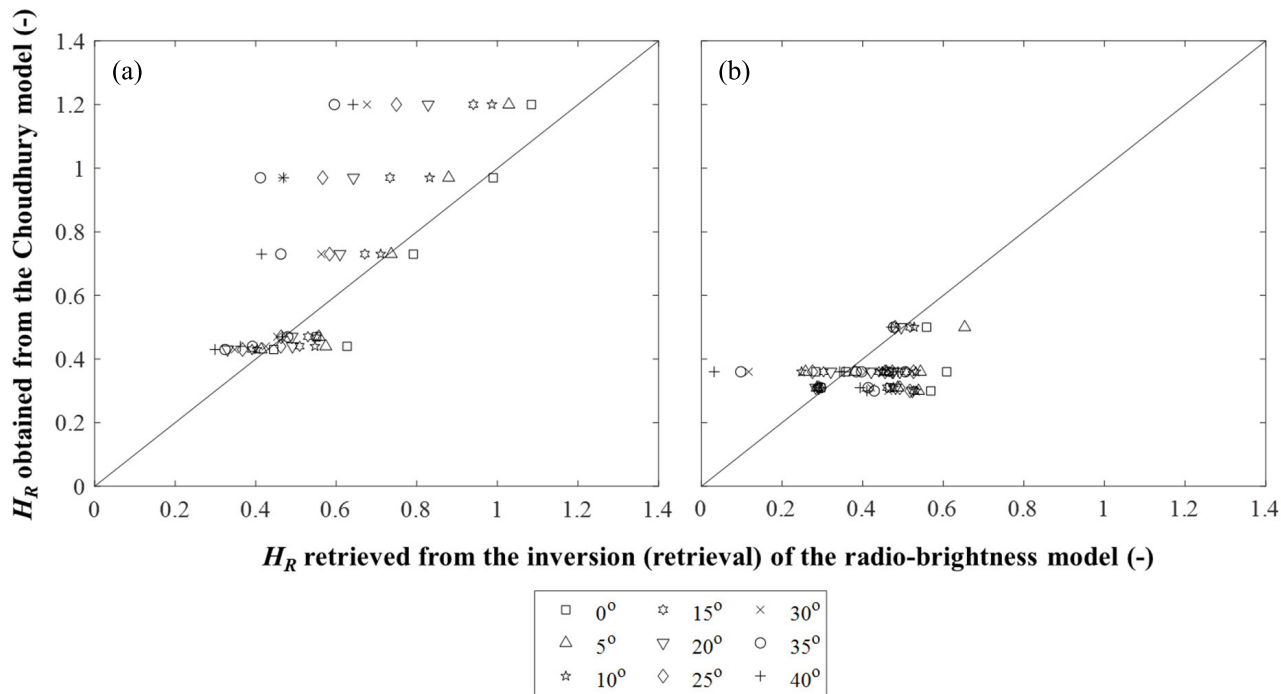


Fig. 8. H_R obtained from the inversion (retrieval) of the radio-brightness model versus from the Choudhury model at 9 different incidence angles (from 0 to 40°) (a) before and (b) after the compaction process.

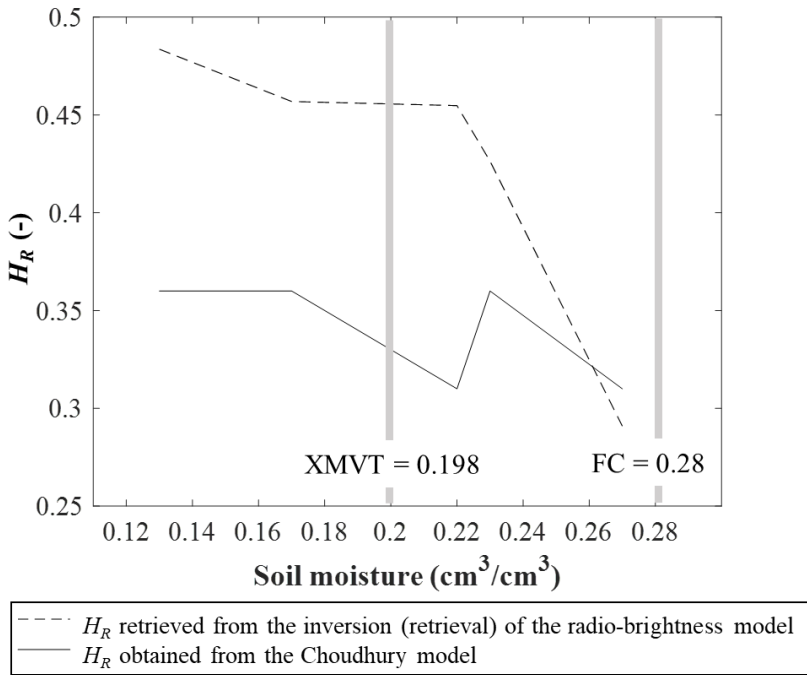


Fig. 9. H_R retrieved from inversion (retrieval) of the radio-brightness model and the Choudhury model compared with changes of SM from dry to wet conditions after the soil is compacted.

the SM accuracy showed an improvement for most incidence angles, with an accuracy of 0.04 cm³/cm³ achieved for all incidence angles, except 0.05 cm³/cm³ at 25° and 30° when using the V polarization. The angle ranges from 0° to 15° gave a somewhat better result than the rest of incidence angles, with

an accuracy of 0.03–0.04 cm³/cm³ when either using dual or V polarization. It can be seen that with the use of the modified H_R model, which includes incidence angle and SM content, the use of dual or V polarization is expected to provide a higher accuracy than using only H polarization, and the SM

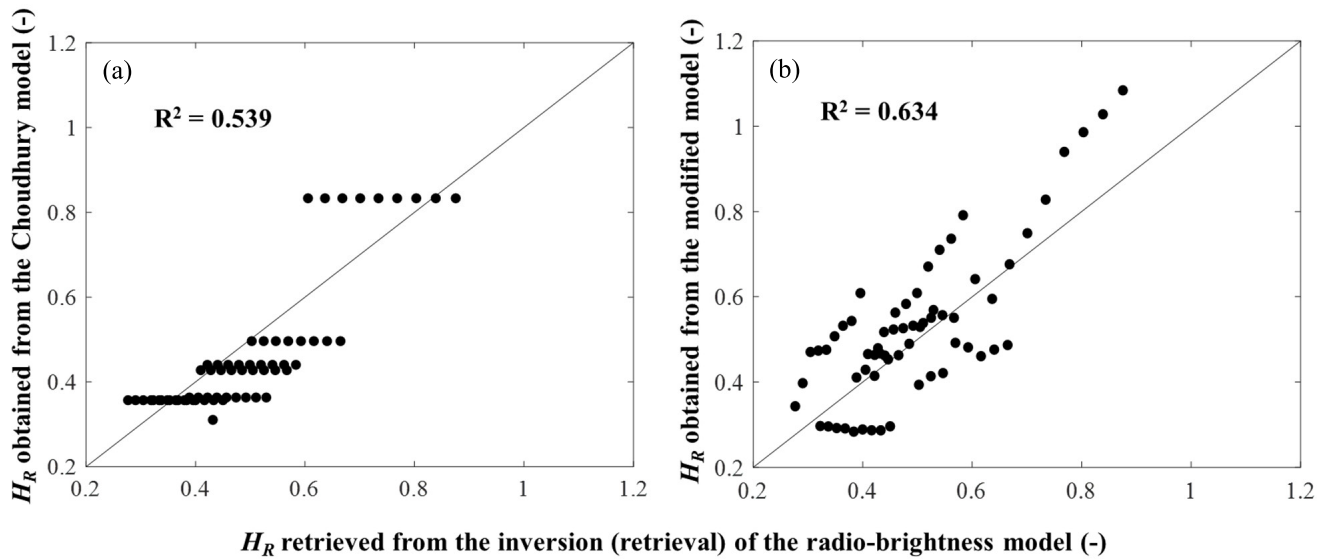


Fig. 10. H_R obtained from the inversion (retrieval) of the radio-brightness model versus H_R obtained from (a) Choudhury model and (b) modified H_R model using the data of the second layer, including before and after compaction and the data after watering on February 2.

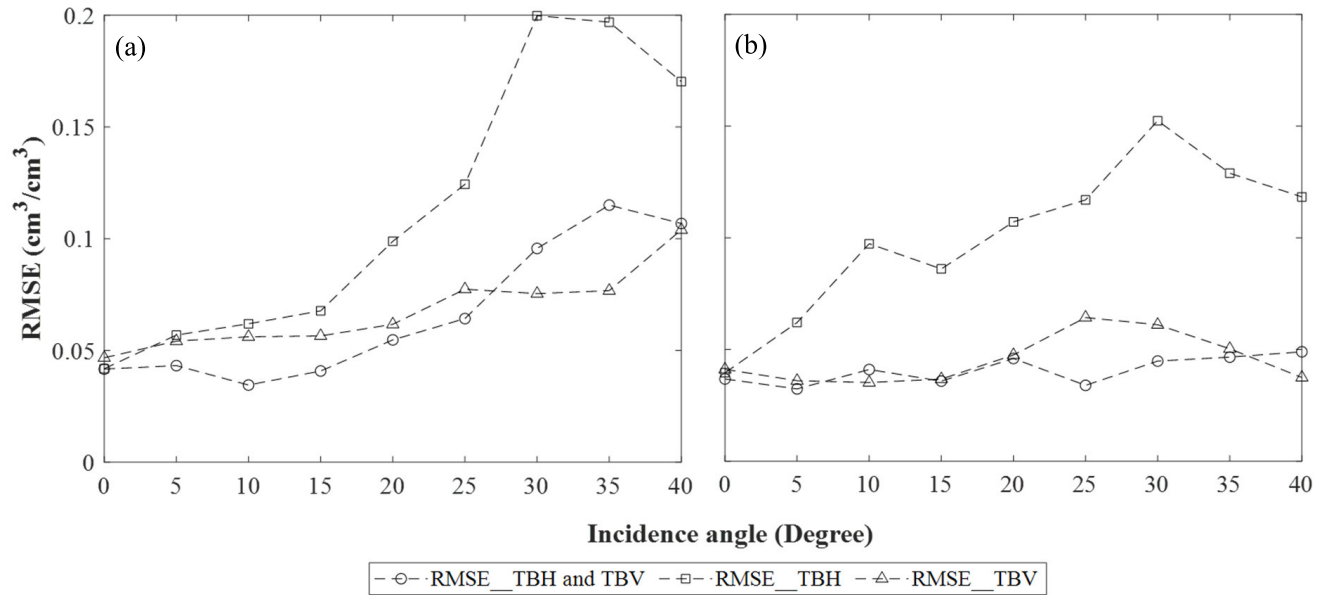


Fig. 11. RMSE of SM retrieval results at different single incidence angles (from 0° to 40°) for six sets of experiments before and after the compaction process of the second layer and after surface watering on February 2 when using (a) constant H_R value from the Choudhury model and (b) H_R values obtained from the modified H_R model.

retrieval results can be obtained with $0.04\text{-cm}^3/\text{cm}^3$ accuracy at almost all incidence angles and this accuracy is most consistent at a range of incidence angle from 0° to 15° .

V. CONCLUSION AND DISCUSSION

The effective surface roughness parameter (H_R) was found to be the most influential factor on SM retrieval results when compared to other factors, with a change of 0.1 in H_R leading to a change of 5 K in TB. Moreover, this factor has different effects on SM retrieval results based on the SM condition and has been shown to be more important in wet conditions. Apart from geometric soil surface roughness, incidence angle and

SM showed the greatest impact on the change of H_R , leading to the need to account for their contribution.

This article has demonstrated an improved accuracy of SM retrieval results by using this new surface roughness parameter (H_R) model. It can be concluded that with this model, which includes the contribution of incidence angle and SM content, the use of dual or V polarization TB observations provided a higher accuracy than using only H polarization, and the SM retrieval results can be obtained with an accuracy of $0.04\text{ cm}^3/\text{cm}^3$ over almost all incidence angles except $0.05\text{ cm}^3/\text{cm}^3$ at 25° and 30° when using V polarization. This result is consistent with findings from previous studies

showing that using V polarization showed the best SM retrieval performance compared to using H polarization [47]. In addition, based on the footprint of the radiometer on the ground [Fig. 1(b)], it can be seen that the H polarization observation is spread more along the length of the testbed, meaning that there is a wider range of incidence angles. Accordingly, worse performance of H polarization can be explained by the fact that radio-brightness models do not account for a wide range of incidence angles; the use of smaller incidence angles minimizes the range of angles in the footprint.

It was suggested that using dual or single polarization alone at 0° is the recommended configuration for use in further field testing [4]; therefore, the surface roughness parameter (H_R) model developed in this study is reasonable and convincing enough to support an improvement in the accuracy of the SM retrieval result.

Despite the fact that this study is based on the Q/H model to solve the rough surface microwave radiation, it is recommended that the performance of this model can be compared with other models (e.g., AIEM) in order to understand the novelty of the proposed approach. In addition, a local sensitivity analysis was used here to study the effect of one parameter on the model output, while all other parameters remained constant. However, in order to obtain more reliable conclusions, it is recommended that in future studies, the global sensitivity analysis method (e.g., the extended Fourier amplitude sensitivity (EFAST) [48]) can be used, which allows the average response of model output to be examined and its sensitivity quantified when all parameters are varied within a defined range.

ACKNOWLEDGMENT

The authors would like to thank the reviewers and editors for their grateful comments to improve this article. They would like to thank the technical staff at the Department of Civil Engineering, Monash University, Clayton, VIC, Australia. The ELBARA III was provided by the Institute of Bio- and Geosciences, Forschungszentrum Jülich GmbH, Jülich, Germany, and other types of equipment were provided by Prof. Jeff Walker's group. They would also like to thank SPARC Hub members for their moral support throughout the experiments.

REFERENCES

- [1] F. Bayomy, H. Salem, and G. Assistant, "Monitoring and modeling subgrade soil moisture for pavement design and rehabilitation in Idaho phase III: Data collection and analysis," Idaho Transp. Dept., Boise, ID, USA, Tech. Rep., 2004.
- [2] F. T. Ulaby, M. Razani, and M. C. Dobson, "Effects of vegetation cover on the microwave radiometric sensitivity to soil moisture," *IEEE Trans. Geosci. Remote Sens.*, vol. GE-21, no. 1, pp. 51–61, Jan. 1983, doi: [10.1109/TGRS.1983.350530](https://doi.org/10.1109/TGRS.1983.350530).
- [3] M. Schwank et al., "ELBARA II, an L-band radiometer system for soil moisture research," *Sensors*, vol. 10, no. 1, pp. 584–612, Jan. 2010, doi: [10.3390/s100100584](https://doi.org/10.3390/s100100584).
- [4] T. M. Nguyen, J. P. Walker, N. Ye, and J. Kodikara, "Use of an L-band radiometer for proximal moisture measurement in road construction," *Transp. Geotechnics*, vol. 38, Jan. 2023, Art. no. 100876, doi: [10.1016/j.trgeo.2022.100876](https://doi.org/10.1016/j.trgeo.2022.100876).
- [5] Y. H. Kerr, P. Waldteufel, J.-P. Wigneron, J. Martinuzzi, J. Font, and M. Berger, "Soil moisture retrieval from space: The soil moisture and ocean salinity (SMOS) mission," *IEEE Trans. Geosci. Remote Sens.*, vol. 39, no. 8, pp. 1729–1735, Aug. 2001, doi: [10.1109/36.942551](https://doi.org/10.1109/36.942551).
- [6] Y. H. Kerr et al., "The SMOS mission: New tool for monitoring key elements of the global water cycle," in *Proc. IEEE*, vol. 98, no. 5, pp. 666–687, May 2010, doi: [10.1109/JPROC.2010.2043032](https://doi.org/10.1109/JPROC.2010.2043032).
- [7] A. Al-Yaari et al., "Global-scale evaluation of two satellite-based passive microwave soil moisture datasets (SMOS and AMSR-E) with respect to land data assimilation system estimates," *Remote Sens. Environ.*, vol. 149, pp. 181–195, Jun. 2014, doi: [10.1016/j.rse.2014.04.006](https://doi.org/10.1016/j.rse.2014.04.006).
- [8] T. Meyer, L. Weihermüller, H. Vereecken, and F. Jonard, "Vegetation optical depth and soil moisture retrieved from L-band radiometry over the growth cycle of a winter wheat," *Remote Sens.*, vol. 10, no. 10, p. 1637, Oct. 2018, doi: [10.3390/rs10101637](https://doi.org/10.3390/rs10101637).
- [9] T. Jiang, K. Zhao, X. Zheng, S. Chen, and X. Wan, "Dynamic bp in the L band and its role in improving the accuracy of soil moisture retrieval," *Chin. Geographical Sci.*, vol. 29, no. 2, pp. 283–292, Mar. 2019, doi: [10.1007/s11769-019-1028-0](https://doi.org/10.1007/s11769-019-1028-0).
- [10] T. Zhao et al., "Soil moisture retrievals using L-band radiometry from variable angular ground-based and airborne observations," *Remote Sens. Environ.*, vol. 248, Oct. 2020, Art. no. 111958, doi: [10.1016/j.rse.2020.111958](https://doi.org/10.1016/j.rse.2020.111958).
- [11] F. T. Ulaby, R. K. Moore, and A. K. Fung. (Jan. 1986). *Microwave Remote Sensing: Active and Passive. Volume 3—From Theory to Applications*. Accessed: Nov. 28, 2022. [Online]. Available: <https://ntrs.nasa.gov/citations/19860041708>
- [12] A. K. Fung, Z. Li, and K. S. Chen, "Backscattering from a randomly rough dielectric surface," *IEEE Trans. Geosci. Remote Sens.*, vol. 30, no. 2, pp. 356–369, Mar. 1992, doi: [10.1109/36.134085](https://doi.org/10.1109/36.134085).
- [13] K. S. Chen, T.-D. Wu, L. Tsang, Q. Li, J. Shi, and A. K. Fung, "Emission of rough surfaces calculated by the integral equation method with comparison to three-dimensional moment method simulations," *IEEE Trans. Geosci. Remote Sens.*, vol. 41, no. 1, pp. 90–101, Jan. 2003, doi: [10.1109/TGRS.2002.807587](https://doi.org/10.1109/TGRS.2002.807587).
- [14] M. Neelam, A. Colliander, B. P. Mohanty, M. H. Cosh, S. Misra, and T. J. Jackson, "Multiscale surface roughness for improved soil moisture estimation," *IEEE Trans. Geosci. Remote Sens.*, vol. 58, no. 8, pp. 5264–5276, Aug. 2020, doi: [10.1109/TGRS.2019.2961008](https://doi.org/10.1109/TGRS.2019.2961008).
- [15] J. R. Wang and B. J. Choudhury, "Remote sensing of soil moisture content, over bare field at 1.4 GHz frequency," *J. Geophys. Res.*, vol. 86, no. C6, p. 5277, 1981, doi: [10.1029/jc086ic06p05277](https://doi.org/10.1029/jc086ic06p05277).
- [16] J.-P. Wigneron et al., "L-band microwave emission of the biosphere (L-MEB) Model: Description and calibration against experimental data sets over crop fields," *Remote Sens. Environ.*, vol. 107, no. 4, pp. 639–655, Apr. 2007, doi: [10.1016/j.rse.2006.10.014](https://doi.org/10.1016/j.rse.2006.10.014).
- [17] J. R. Wang, P. E. O'Neill, T. J. Jackson, and E. T. Engman, "Multifrequency measurements of the effects of soil moisture, soil texture, and surface roughness," *IEEE Trans. Geosci. Remote Sens.*, vol. GE-21, no. 1, pp. 44–51, Jan. 1983, doi: [10.1109/TGRS.1983.350529](https://doi.org/10.1109/TGRS.1983.350529).
- [18] T. Mo and T. J. Schmugge, "A parameterization of the effect of surface roughness on microwave emission," *IEEE Trans. Geosci. Remote Sens.*, vols. GE-25, no. 4, pp. 481–486, Jul. 1987, doi: [10.1109/TGRS.1987.289860](https://doi.org/10.1109/TGRS.1987.289860).
- [19] J. P. Wigneron, L. Laguerre, and Y. H. Kerr, "A simple parameterization of the L-band microwave emission from rough agricultural soils," *IEEE Trans. Geosci. Remote Sens.*, vol. 39, no. 8, pp. 1697–1707, Aug. 2001, doi: [10.1109/36.942548](https://doi.org/10.1109/36.942548).
- [20] M. J. Escorihuela, Y. H. Kerr, P. D. Rosnay, J. P. Wigneron, J. C. Calvet, and F. Lemaitre, "A simple model of the bare soil microwave emission at L-band," *IEEE Trans. Geosci. Remote Sens.*, vol. 45, no. 7, pp. 1978–1987, Jul. 2007, doi: [10.1109/TGRS.2007.894935](https://doi.org/10.1109/TGRS.2007.894935).
- [21] K. Saleh et al., "Estimates of surface soil moisture under grass covers using L-band radiometry," *Remote Sens. Environ.*, vol. 109, no. 1, pp. 42–53, Jul. 2007, doi: [10.1016/j.rse.2006.12.002](https://doi.org/10.1016/j.rse.2006.12.002).
- [22] R. Panciera, J. P. Walker, and O. Merlin, "Improved understanding of soil surface roughness parameterization for L-band passive microwave soil moisture retrieval," *IEEE Geosci. Remote Sens. Lett.*, vol. 6, no. 4, pp. 625–629, Oct. 2009, doi: [10.1109/LGRS.2009.2013369](https://doi.org/10.1109/LGRS.2009.2013369).
- [23] B. J. Choudhury, T. J. Schmugge, A. Chang, and R. W. Newton, "Effect of surface roughness on the microwave emission from soils," *J. Geophys. Res.*, vol. 84, no. C9, p. 5699, 1979, doi: [10.1029/jc084ic09p05699](https://doi.org/10.1029/jc084ic09p05699).
- [24] J.-P. Wigneron et al., "Evaluating an improved parameterization of the soil emission in L-MEB," in *IEEE Trans. Geosci. Remote Sens.*, vol. 49, no. 4, pp. 1177–1189, Apr. 2011, doi: [10.1109/TGRS.2010.2075935](https://doi.org/10.1109/TGRS.2010.2075935).
- [25] A. Mialon, J.-P. Wigneron, P. de Rosnay, M. J. Escorihuela, and Y. H. Kerr, "Evaluating the L-MEB model from long-term microwave measurements over a rough field, SMOSREX 2006," *IEEE Trans. Geosci. Remote Sens.*, vol. 50, no. 5, pp. 1458–1467, May 2012, doi: [10.1109/TGRS.2011.2178421](https://doi.org/10.1109/TGRS.2011.2178421).

- [26] J. Wang et al., "Microwave radiometer experiment of soil moisture sensing at BARC test site during summer 1981," NASA Goddard Space Flight Center, Greenbelt, MD, USA, Tech. Memo 86056, 1984.
- [27] U. Wegmuller and C. Matzler, "Rough bare soil reflectivity model," *IEEE Trans. Geosci. Remote Sens.*, vol. 37, no. 3, pp. 1391–1395, May 1999, doi: [10.1109/36.763303](https://doi.org/10.1109/36.763303).
- [28] H. Lawrence, J.-P. Wigneron, F. Demontoux, A. Mialon, and Y. H. Kerr, "Evaluating the semiempirical H–Q model used to calculate the L-band emissivity of a rough bare soil," *IEEE Trans. Geosci. Remote Sens.*, vol. 51, no. 7, pp. 4075–4084, Jul. 2013, doi: [10.1109/TGRS.2012.2226995](https://doi.org/10.1109/TGRS.2012.2226995).
- [29] M. A. Goodberlet and J. B. Mead, "A model of surface roughness for use in passive remote sensing of bare soil moisture," *IEEE Trans. Geosci. Remote Sens.*, vol. 52, no. 9, pp. 5498–5505, Sep. 2014, doi: [10.1109/TGRS.2013.2289979](https://doi.org/10.1109/TGRS.2013.2289979).
- [30] T. Zhao et al., "Parametric exponentially correlated surface emission model for L-band passive microwave soil moisture retrieval," *Phys. Chem. Earth, A/B/C*, vols. 83–84, pp. 65–74, Jan. 2015, doi: [10.1016/j.pce.2015.04.001](https://doi.org/10.1016/j.pce.2015.04.001).
- [31] M. Rafiq, "Soil variability in agronomic research," *Pakistan J. Soil Sci.*, vol. 5, nos. 1–2, pp. 9–14, 1992.
- [32] M. Mahmood-ul-Hassan and P. J. Gregory, "Water transmission properties as affected by cropping and tillage systems," *Pakistan J. Soil Sci.*, vol. 16, nos. 1–2, pp. 29–38, 1999.
- [33] Y. Oh and Y. C. Kay, "Condition for precise measurement of soil surface roughness," *IEEE Trans. Geosci. Remote Sens.*, vol. 36, no. 2, pp. 691–695, Mar. 1998, doi: [10.1109/36.662751](https://doi.org/10.1109/36.662751).
- [34] M. W. J. Davidson, T. L. Toan, F. Mattia, G. Satalino, T. Manninen, and M. Borgeaud, "On the characterization of agricultural soil roughness for radar remote sensing studies," *IEEE Trans. Geosci. Remote Sens.*, vol. 38, no. 2, pp. 630–640, Mar. 2000, doi: [10.1109/36.841993](https://doi.org/10.1109/36.841993).
- [35] C. Matzler et al., "ELBARA, the ETH L-band radiometer for soil-moisture research," in *Proc. IEEE Int. Geosci. Remote Sens. Symp. (IGARSS)*, vol. 5, Jul. 2003, pp. 3058–3060, doi: [10.1109/IGARSS.2003.1294682](https://doi.org/10.1109/IGARSS.2003.1294682).
- [36] Y. Oh, K. Sarabandi, and F. T. Ulaby, "An empirical model and an inversion technique for radar scattering from bare soil surfaces," *IEEE Trans. Geosci. Remote Sens.*, vol. 30, no. 2, pp. 370–381, Mar. 1992, doi: [10.1109/36.134086](https://doi.org/10.1109/36.134086).
- [37] H. A. K. M. Bhuiyan et al., "Assessing SMAP soil moisture scaling and retrieval in the Carman (Canada) study site," *Vadose Zone J.*, vol. 17, no. 1, 2018, Art. no. 180132, doi: [10.2136/vzj2018.07.0132](https://doi.org/10.2136/vzj2018.07.0132).
- [38] A. Fresnel, "Note sur le calcul des teintes que la polarisation développe dans les lames cristallisées," *Annales de Chimie et Physique*, vol. 17, pp. 101–112, 1821.
- [39] M. C. Dobson, F. T. Ulaby, M. T. Hallikainen, and M. A. El-Rayes, "Microwave dielectric behavior of wet soil-part II: Dielectric mixing models," *IEEE Trans. Geosci. Remote Sens.*, vol. GE-23, no. 1, pp. 35–46, Jan. 1985, doi: [10.1109/TGRS.1985.289498](https://doi.org/10.1109/TGRS.1985.289498).
- [40] B. J. Choudhury, T. J. Schmugge, and T. Mo, "A parameterization of effective soil temperature for microwave emission," *J. Geophys. Res.*, vol. 87, no. C2, p. 1301, 1982, doi: [10.1029/jc087ic02p01301](https://doi.org/10.1029/jc087ic02p01301).
- [41] J.-P. Wigneron, J.-C. Calvet, T. Pellarin, A. A. Van de Griend, M. Berger, and P. Ferrazzoli, "Retrieving near-surface soil moisture from microwave radiometric observations: Current status and future plans," *Remote Sens. Environ.*, vol. 85, no. 4, pp. 489–506, Jun. 2003, doi: [10.1016/S0034-4257\(03\)00051-8](https://doi.org/10.1016/S0034-4257(03)00051-8).
- [42] Y. H. Kerr et al., "The SMOS soil moisture retrieval algorithm," *IEEE Trans. Geosci. Remote Sens.*, vol. 50, no. 5, pp. 1384–1403, May 2012, doi: [10.1109/TGRS.2012.2184548](https://doi.org/10.1109/TGRS.2012.2184548).
- [43] S. Peischl, J. P. Walker, D. Ryu, Y. H. Kerr, R. Panciera, and C. Rudiger, "Wheat canopy structure and surface roughness effects on multiangle observations at L-band," *IEEE Trans. Geosci. Remote Sens.*, vol. 50, no. 5, pp. 1498–1506, May 2012, doi: [10.1109/TGRS.2011.2174644](https://doi.org/10.1109/TGRS.2011.2174644).
- [44] B. Peng et al., "Reappraisal of the roughness effect parameterization schemes for L-band radiometry over bare soil," *Remote Sens. Environ.*, vol. 199, pp. 63–77, Sep. 2017, doi: [10.1016/j.rse.2017.07.006](https://doi.org/10.1016/j.rse.2017.07.006).
- [45] A. Y. Bai et al., "A multi-temporal and multi-angular approach for systematically retrieving soil moisture and vegetation optical depth from SMOS data," *Remote Sens. Environ.*, vol. 280, Oct. 2022, Art. no. 113190, doi: [10.1016/j.rse.2022.113190](https://doi.org/10.1016/j.rse.2022.113190).
- [46] Y. H. Kerr et al., "SMOS level 2 soil moisture processor development continuation project," Algorithm Theor. Basis Doc, Tech. Note SO-TN-ARR-L2PP 0037, 2011, vol. 3, no. 4, p. 121. [Online]. Available: <https://earth.esa.int/eogateway/documents/20142/37627/SMOS-L2-SM-ATBD.pdf>
- [47] S. K. Chan et al., "Development and assessment of the SMAP enhanced passive soil moisture product," *Remote Sens. Environ.*, vol. 204, pp. 931–941, Jan. 2018, doi: [10.1016/j.rse.2017.08.025](https://doi.org/10.1016/j.rse.2017.08.025).



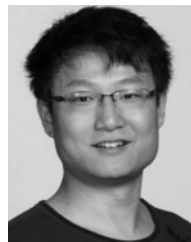
Thi Mai Nguyen (Graduate Student Member, IEEE) received the B.E. degree in geography from the Hanoi University of Science, Hanoi, Vietnam, in 2017, and the M.Sc. degree in remote sensing and geographic information system (GIS) from National Central University, Taoyuan, Taiwan, in 2019. She is currently pursuing the Ph.D. degree in civil engineering with Monash University, Clayton, VIC, Australia. Her Ph.D. thesis aims at developing a method for proximately monitoring the spatial variation of soil moisture in road construction using an L-band radiometer.



Jeffrey P. Walker (Fellow, IEEE) received the B.E. degree in civil engineering, the Bachelor of Surveying degree (Hons.), and the Ph.D. degree in water resources engineering from The University of Newcastle, Callaghan, NSW, Australia, in 1995, 1995, and 1999, respectively.

He joined the National Aeronautics and Space Administration (NASA) Goddard Space Flight Centre, Greenbelt, MD, USA, in 1999, to implement his soil moisture (SM) work globally. In 2001, he joined the Department of Civil and Environmental Engineering, The University of Melbourne, Melbourne, VIC, Australia, as a Lecturer. Since 2010, he has been a Professor with the Department of Civil Engineering, Monash University, Clayton, VIC, USA, where he is continuing his research. He is contributing to SM satellite missions at NASA, European Space Agency (ESA), and JAXA, as a Science Team Member for the Soil Moisture Active Passive Mission and a Cal/Val Team Member for the Soil Moisture and Ocean Salinity and Global Change Observation Mission—Water, respectively.

Dr. Walker received the University Medal for Bachelor of Surveying from The University of Newcastle.



Nan Ye (Member, IEEE) received the B.E. degree in hydraulic and hydropower engineering from Tsinghua University, Beijing, China, in 2006, and the Ph.D. degree in civil engineering from Monash University, Clayton, VIC, Australia, in 2014.

He coordinated a number of airborne field experiments for the in-orbit calibration/validation of the Soil Moisture Active Passive Mission in the Murrumbidgee River catchment, Southeast of Australia. He is a Senior Research Fellow with Monash University, working on P-band passive microwave remote sensing of soil moisture.



Jayantha Kodikara received the B.E. degree from the University of Peradeniya, Central, Sri Lanka, in 1983, and the Ph.D. degree in geotechnical engineering from Monash University, Clayton, VIC, Australia, in 1989. His Ph.D. thesis was on the side resistance development of piles socketed into Melbourne mudstone.

He worked on a finite-element analysis of soil–structure interaction problems, as a Post-Doctoral Research Fellow at The University of Newcastle, Callaghan, NSW, Australia, from 1989 to 1991. He worked as a Senior Geotechnical Engineer with Golder Associates Pty. Ltd., Melbourne, VIC, Australia, from 1991 to 1994. After joining Monash University in 2001, he has developed vigorous research programs into both fundamental and applied research in civil engineering. He is also the Technical Leader of global project on Advanced Condition Assessment and Pipe Failure Prediction Project.

Dr. Kodikara is a fellow of the Institution of Engineers Australia and a Chartered Professional Engineer in Australia and an Associate Editor of *Canadian Geotechnical Journal* and the *Journal of Environmental Geotechnics*.